EISEVIER

Contents lists available at ScienceDirect

### Ecotoxicology and Environmental Safety

journal homepage: www.elsevier.com/locate/ecoenv



## Biological effects of four iron-containing nanoremediation materials on the green alga *Chlamydomonas* sp.



Nhung H.A. Nguyen<sup>a</sup>, Nadia R. Von Moos<sup>b</sup>, Vera I. Slaveykova<sup>b,\*</sup>, Katrin Mackenzie<sup>c</sup>, Rainer U. Meckenstock<sup>d</sup>, Silke Thűmmler<sup>e</sup>, Julian Bosch<sup>f,1</sup>, Alena Ševců<sup>a,\*</sup>

- <sup>a</sup> Technical University of Liberec, Institute for Nanomaterials, Advanced Technologies and Innovation, Faculty of Mechatronics, Informatics and Multidisciplinary Studies, Studentská 2. 461 17 Liberec, Czech Republic
- b University of Geneva, Faculty of Sciences, Earth and Environmental Sciences, Department for Environmental and Aquatic Sciences, Uni Carl Vogt, 66 Bvd Carl Vogt, 1211 Geneva, Switzerland
- <sup>c</sup> Helmholtz Centre for Environmental Research GmbH-UFZ, Permoserstraße 15, 04318 Leipzig, Germany
- <sup>d</sup> University of Duisburg-Essen, Biofilm Centre, Universitätsstr. 5, 45141 Essen, Germany
- e TU Bergakademie Freiberg, Institute of Mechanical Process Engineering and Mineral Processing, Agricolastraße 1, 09599 Freiberg, Germany
- f Helmholtz Zentrum München, Ingolstädter Landstraße 1, 85764 Neuherberg, Germany

#### ARTICLE INFO

# Keywords: Biological effect FerMEG12 Carbo-Iron Trap-Ox Fe-zeolite Nano-Goethite Chlamydomonas sp.

#### ABSTRACT

As nanoremediation strategies for in-situ groundwater treatment extend beyond nanoiron-based applications to adsorption and oxidation, ecotoxicological evaluations of newly developed materials are required. The biological effects of four new materials with different iron (Fe) speciations ([i] FerMEG12 - pristine flake-like milled Fe(0) nanoparticles (nZVI), [ii] Carbo-Iron\* - Fe(0)-nanoclusters containing activated carbon (AC) composite, [iii] Trap-Ox® Fe-BEA35 (Fe-zeolite) - Fe-doped zeolite, and [iv] Nano-Goethite - 'pure' FeOOH) were studied using the unicellular green alga Chlamydomonas sp. as a model test system. Algal growth rate, chlorophyll fluorescence, efficiency of photosystem II, membrane integrity and reactive oxygen species (ROS) generation were assessed following exposure to 10, 50 and 500 mg L<sup>-1</sup> of the particles for 2 h and 24 h. The particles had a concentration-, material- and time-dependent effect on Chlamydomonas sp., with increased algal growth rate after 24 h. Conversely, significant intracellular ROS levels were detected after 2 h, with much lower levels after 24 h. All Fe-nanomaterials displayed similar Z-average sizes and zeta-potentials at 2 h and 24 h. Effects on Chlamydomonas sp. decreased in the order FerMEG12 > Carbo-Iron® > Fe-zeolite > Nano-Goethite. Ecotoxicological studies were challenged due to some particle properties, i.e. dark colour, effect of constituents and a tendency to agglomerate, especially at high concentrations. All particles exhibited potential to induce significant toxicity at high concentrations (500 mg L<sup>-1</sup>), though such concentrations would rapidly decrease to mg or  $\mu$ g L<sup>-1</sup> in aquatic environments, levels harmless to *Chlamydomonas* sp. The presented findings contribute to the practical usage of particle-based nanoremediation in environmental restoration.

#### 1. Introduction

Iron (Fe)-based materials possess remarkable potential for the remediation of soil aquifers, groundwater and cyanobacterial blooms (Bardos et al., 2015; Ribas et al., 2016; Sharma et al., 2016). Numerous in-situ applications of zero-valent iron (ZVI) nanoparticles have proved a powerful tool in the clean-up of chlorinated ethenes and toxic metal

ions due to their high reductive capacity (Köber et al., 2014; Mueller et al., 2012). Further, emerging particulate materials containing Fe as Fe(0), Fe(II) and Fe(III), where the Fe species act as reductants or sorbents for metals and metalloids, have been used successfully in microbiological contaminant degradation or as heterogeneous Fenton catalysts (Bardos et al., 2015; Mackenzie et al., 2016; Gillies et al., 2017).

Abbreviations: AC, activated carbon; DLS, dynamic light scattering; FCM, flow cytometry; FE SEM, field-emission scanning electron microscopy; FU, fluorescence units; nZVI, nanoscale zero-valent iron; ORP, oxidative reductive potential; PI, propidium iodide; PSII, photosystem II; QY, quantum yield; ROS, reactive oxygen species; ZVI, zero-valent iron

E-mail addresses: nhung.nguyen@tul.cz (N.H.A. Nguyen), nadia.vonmoos@immerda.ch (N.R. Von Moos), vera.slaveykova@unige.ch (V.I. Slaveykova), katrin.mackenzie@ufz.de (K. Mackenzie), rainer.meckenstock@uni-due.de (R.U. Meckenstock), Silke.Thuemmler@mvtat.tu-freiberg.de (S. Thűmmler), julian.bosch@intrapore.com (J. Bosch), alena.sevcu@tul.cz (A. Ševců).

<sup>\*</sup> Corresponding authors.

Present address: Intrapore UG, Katernberger Str. 107, 45327 Essen, Germany.

The overall impact of materials containing Fe(0) on aquatic ecosystems (introduced intentionally or accidentally) remains questionable (Bardos et al., 2015). Other nanomaterials also have the potential to seriously affect aquatic microorganisms such as microalgae, primary producers that play a key role in healthy ecosystems (Adeleye et al., 2016; Klaine et al., 2008). While iron is an essential nutrient in small amounts, increased loading of Fe(II)/Fe(III) ions can rapidly accumulate in the cells of aquatic organisms, resulting in oxidative stress due to the generation of oxide and hydroxide radicals via the Fenton reaction (Crane and Scott, 2012; Davies et al., 2000; Franqueira et al., 2000; Gillies et al., 2016). Moreover, ZVI particles show a strong affinity for cell surfaces; thus, they have the potential to physically damage bacterial or algal cells (Auffan et al., 2008; Lei et al., 2016).

A number of Fe-containing materials have been developed under the European FP7 project NanoRem (for more information see nanorem.eu) in order to provide new and improved materials for treatment of contaminated environments from a broader contaminant spectrum and to offer improved cost effectiveness and safety during transportation and application (Bardos et al., 2015). Up to now, nanoremediation using insitu generation of permeable reactive barriers or zones through particle subsurface injection has been dominated by nanoiron-based materials. With the introduction of particles with different abilities, nanoremediation has been extended to support bioremediation, advanced oxidation and sorption-assisted clean-up strategies in permeable barriers.

During large-scale in-situ applications, such as those reported for ZVI injection for the treatment of chlorinated organic contaminants (Mueller et al., 2012; Soukupova et al., 2015), suspensions containing up to  $10\,\mathrm{g\,L}^{-1}$  of particles are typically injected. Following migration of in-situ applied nanoscale ZVI (nZVI) suspensions within the treated aquifer or water body, Fe concentrations are expected to decline to  $\mathrm{mg\,L}^{-1}$  levels or lower (Mueller et al., 2012); hence, ecotoxicological studies should be aimed at such concentrations.

The present study attempts to assess the biological effects of such Fe-containing materials on an aquatic microorganism commonly found in fresh water and soils, *Chlamydomonas* sp., using multiple biological end-points, i.e. growth rate, chlorophyll fluorescence, photosystem II (PSII) quantum efficiency, membrane integrity and intracellular reactive oxygen species (ROS) generation. The algal system was chosen as it is usually associated with contact effects to the cell wall rather than particle incorporation. In addition, behaviour of the Fe-containing materials in the exposure medium was characterised in terms of size, zeta-potential and effect on pH and oxidative reductive potential (ORP).

#### 2. Material and methods

#### 2.1. Fe-containing materials

Four newly developed Fe-containing materials intended for subsurface application as suspensions were examined (see Table 1 for particle descriptions and an overview of their constituents and intended use). The materials were received as dry powders and suspended according to the producers' instructions.

 $\it FerMEG12$  are metallic ZVI particles that are produced mechanically using a two-stage top-down process and are one of the emerging particles for in-situ groundwater reduction (Köber et al., 2014). Particles of  $<40\,\mu m$  were first generated by dry milling and then more finely ground by wet milling in bivalent alcohol. The milling process forms nanostructured flake-shaped particles.

Carbo-Iron\* is a composite of ZVI-nanostructures embedded in activated carbon (AC) particles of about 1  $\mu$ m. Carbo-Iron\* was synthesised carbothermally following a wet impregnation step, where the pores of the colloidal AC particles are filled with ferric nitrate (Fe (NO<sub>3</sub>)<sub>3</sub>) (Bleyl et al., 2012). Electron microscopy following reduction indicates nZVI clusters of predominantly  $d_{Fe} \approx 50$  nm built into the AC grain (Mackenzie et al., 2012).

Fe-zeolites is a porous Fe-exchanged alumosilicate mineral particles of the beta-zeolite type with 1.3 wt% total Fe (Gillies et al., 2017) that catalytically activate oxidising agents such as hydrogen peroxide ( $H_2O_{2j}$  (Gonzalez-Olmos et al., 2013). With a specific surface area of  $602\,\mathrm{m}^2\,\mathrm{g}^{-1}$  ( $N_2$ -BET) and a water-filled pore effective density of  $\rho\approx 1.7\,\mathrm{g\,cm}^{-3}$ , the particles show favourable sedimentation behaviour (i.e. 11– $15\,\mathrm{mm\,h}^{-1}$ ) for in-situ application (Gillies et al., 2016, 2017).

*Nano-Goethite* is produced using an industrial FeOOH precursor that undergoes ultrasonification and coating with a layer of a natural organic polymer that results in electro-steric stabilisation (Bosch et al., 2010; Braunschweig et al., 2013). A stable stock suspension of  $100 \, \mathrm{g \, L^{-1}}$  Nano-Goethite with a mean particle size of 400 nm can be generated in this way.

The shape and particle size of the Fe-containing materials were determined using a Zeiss Ultra Plus field-emission scanning electron microscope (FE SEM). Samples were fixed to aluminium stubs using double-sided carbon tape and cleaned with RF plasma (Evactron) for 10 min before image acquisition. For further details, see Supporting information Fig. S1.

Suspension stabilisers are added in order to generate suspensions stable enough to be injected without major agglomeration (Table 1), carboxymethyl cellulose being added to the FerMEG12 and Carbo-Iron® suspensions and a humic-acid coating used for Nano-Goethite. No stabiliser was added to Fe-zeolites, as it forms a stable suspension.

## 2.2. Characterisation of Fe-containing materials in the algal exposure medium

The hydrodynamic diameter of each particle type was determined at a range of suspension concentrations (10, 50 and 500 mg  $\rm L^{-1})$  in algal growth medium through dynamic light scattering (DLS) using a Malvern Zetasizer Nano ZS (Malvern Instruments, UK) with a 633 nm laser source and a detection angle of 173°. The same instrument was used to measure electrophoretic mobility, which was subsequently transformed to zeta potential using Smoluchowski's approximation. Each sample was measured in triplicate at 30 s intervals. At the beginning and end of each toxicity test, ORP and pH were measured using a standard multimeter (WTW, Germany).

#### 2.3. Algal cultures and exposure conditions

The *Chlamydomonas* sp. used in this study (originally isolated from the Lipno reservoir, Czech Republic) was obtained from the Biology Centre of the Czech Academy of Sciences. The algae were cultivated in Guillard-Lorenzen medium (Guillard and Lorenzen, 1972) (Table S1) in an incubator (PlunoTech, Czech Republic) with a 150 rpm shaker and temperature set to 22  $\pm$  2°C, applying a light: dark regime of 16:8 h with light intensity set to 1200 lux. The culture was harvested during its exponential growth phase and re-suspended in the exposure media to a cell density of 1  $\times$  10 $^6$  cells mL $^{-1}$ .

Based on preliminary experiments, where  $5 \text{ mg L}^{-1}$  of Fe-containing material showed no effect and 1000 mg L<sup>-1</sup> interfered with measurement, toxicological effect was assessed through exposure to 10, 50 and 500 mg L<sup>-1</sup> for 2 and 24 h. The experiments were carried out in fully light-transmitting plastic vials containing 5 mL of Chlamydomonas sp. and the particle suspension. Negative controls without particles were run in parallel. Exposure experiments were performed under the same conditions (light, temperature and agitation regimes) as those described for the stock algal culture. Possible effects due to shading and particle sedimentation were also considered, particularly as high material concentrations produced a dark (FerMEG12 and Carbo-Iron®; Figs. S2 and S3), skimmed milk-like (Fe-zeolites; Fig. S3) or light brown-red (Nano-Goethite; Fig. S3) suspension. After 2 h and 24 h exposure, 250 μL sub-samples were taken and examined through flow cytometry (FCM) in order to assess algal cell number, cellular membrane integrity and chlorophyll fluorescence. The effect on the ROS generation and

 Table 1

 New "nanoremediation" materials for in-situ application in groundwater treatment: summary of particle properties.

Particle type	FerMEG12	Carbo-Iron®	Trap-Ox® Fe-Zeolite	Nano-Goethite
Schematic presentation	(Fe(0)	Fe(0) In activated carbon	(a)	humic acid
Brief description	Flake-like iron (Fe) nanoparticles formed by mechanical milling	Composite material of iron nanoclusters embedded in activated carbon (AC)	Fe-exchanged colloidal beta zeolite	Humic-acid coated nano-sized goethite particles
Composition	Fe metal with thin oxide shell	55 wt% porous AC, with 20 $\pm$ 1 wt% Fe(0) as nano-structures within the AC, 30.3 $\pm$ 1.5 wt% Fe $_{\rm total}$ ,	Porous aluminosilicate (Si <sub>x</sub> Al <sub>y</sub> O <sub>z</sub> with 38% Si and 1.8% Al) with lattice sites exchanged with Fe (II/III)	<b>FeOOH</b>
Main Fe speciation Other constituents	$Fe(0) \approx 80 \text{ wt\%}$ Remains of glycol from milling process	Fe(0) $\approx 20  \text{wt\%}$ Remains of $\approx 10  \text{wt\%}$ built-in Fe(II/III)-oxides	$Fe(II/III) \approx 1.3 \text{ wt}\%$	Fe(III) $\approx 60 \text{ wt}\%$ Humic acid coating
Mean particle size Specific surface area (N <sub>2</sub> BET)	$< 40 \mu m$ , $< 100 nm thick$ $13 - 18 m^2/g$	$1\mu\mathrm{m}$ $550-650\mathrm{m}^2/\mathrm{g}$	$500\mathrm{nm}$ $600\mathrm{m}^2/\mathrm{g}$	$400  \mathrm{nm}$ $135  \mathrm{m^2/g}$
Shape Intended target application	flakes In-situ application as reducing agent	sphere-like fragments In-situ application as combined adsorber and reducing agent	spheres In-situ heterogeneous Fenton catalyst	sphere-like fragments In-situ material for metal adsorption and support of Fereducing bacteria
Additives during application for suppression of particle	e.g. Carboxymethyl cellulose (CMC) as suspension stabiliser	CMC forming a layer around particles that washes off over time	Injection possible without stabiliser	Humic acid coating acts as stabiliser
Provider within the NanoRem project	UVR-FIA GmbH, Germany	SciDre GmbH, Germany	Helmholtz Centre for Environmental Research – UFZ, Germany	University of Duisburg-Essen
References for more information	Köber et al. (2014)	Bleyl et al. (2012), Mackenzie et al. (2012), Mackenzie et al. (2016)	Gillies et al. (2016), Gillies et al. (2017)	Bosch et al. (2010), Braunschweig et al. (2013)

algal PSII was also determined.

#### 2.4. Determination of particle effect on membrane integrity and growth rate

A 250 µL aliquot of each sample was transferred to a Microtiter® 96well flat-bottomed plate and Sytox Green or propidium iodide (PI) fluorescent probes (Life Technologies, Switzerland) were added to the sample at final concentrations of  $1\,\mu M$  and  $7\,\mu M$ , respectively. These probes stain the DNA of affected cells by penetrating impaired cell membranes. The plates were incubated in the dark for 20 min before FCM measurement. Each algal suspension was then passed through a BD Accuri C6 Flow Cytometer (BD Biosciences, USA) with a blue 488 nm excitation laser. Green fluorescence of Sytox Green was measured using the 533/30 nm FL1 channel, red fluorescence of PI using the 585/40 nm FL2 channel and red chlorophyll autofluorescence using the > 670 nm FL3 channel. Cells treated in hot water (100 °C) for 15 min were used as a positive control to test whether the Fe-containing materials interfered with probe staining (Fig. S4). Unexposed algae stained with a fluorescent probe were also included as a negative control. One vial was covered with aluminium foil to create dark conditions mimicking the shading effect caused by the dark colour of the Fe materials. Data were analysed using CFlow Plus software (BD Biosciences, USA). The percentage of autofluorescence, cell membrane integrity and PI (Cheloni et al., 2014, 2016) are all illustrated in the FCM analysis section (Figs. S5 and S6). Determination of algal growth rate (cells  $h^{-1}$ ) =  $(N_{24 h} - N_{2 h}) / (24-2 h)$ ; where  $N_{2 h}$  is the number of cells after 2h exposure and  $N_{24h}$  is the number of cells after 24h exposure. Chlamydomonas produces a new generation approximately every 24 h; hence, the algal cell number at inoculation time (0h) and 2h was considered as similar.

#### 2.5. Determination of the effect of particles on intracellular ROS generation

Sub-samples of 200  $\mu$ L were taken after 2 h, 4 h and 24 h and stained with carboxy-H2DCFDA C-400 (Molecular Probes, Thermo Fisher Scientific Inc.). The intracellular ROS staining procedure used followed that detailed in Szivák et al. (2009). Cells were treated with H<sub>2</sub>O<sub>2</sub> (final concentration 100 mM) in a preliminary test to verify the ROS staining procedure. An algal culture without particles was used as a negative control. Fluorescence was measured using a Synergy HTX plate reader (BioTek, USA) with excitation set at 485 nm and emission at 528 nm. The results are presented as the ratio between fluorescence units (FU) in the presence of particles (FU<sub>E</sub>) versus FU for controls without particles (FU<sub>0</sub>): FU<sub>E</sub>/FU<sub>0</sub>.

#### 2.6. Determination of particle effect on PSII

Suspensions of the all particle types were added to the same algal cultures (cell density approximately  $1 \times 10^6$  cells mL<sup>-1</sup>) in 30 mL glass flasks in order to achieve final concentrations of 50 and 100 mg L<sup>-1</sup>of FerMEG12 and Carbo-Iron $^{\circ}$ , and 50, 100 and 500 mg L $^{-1}$  of Fe-zeolites and Nano-Goethite. An algal culture without particles was used as a negative control and incubated in the dark, mimicking the dark colour of the materials. Aliquots (2.2 mL) of each sample were taken immediately and after 24 h incubation to determine their effect on the PSII quantum yield (PSII QY) using an AquaPen-C AP-C 100 fluorometer (PSI Ltd., Czech Republic). All measurements were dark-adapted for 5 min and undertaken in triplicate. QY, which represents the ratio of variable fluorescence ( $F_v = F_m - F_0$ ) to maximum fluorescence ( $F_m$ ): QY = F<sub>v</sub>:F<sub>m</sub>, is used as a proxy of photochemical quenching efficiency (Maxwell and Johnson, 2000). F<sub>m</sub> was obtained by applying illumination (3000  $\mu$ mol photons m<sup>-2</sup> s<sup>-1</sup>) at 680 nm for a few seconds, with minimal fluorescence (Fo; the initial measurement at minimum fluorescence levels in the absence of photosynthetic light) determined at 50 μs.

#### 2.7. Optical microscopy

Untreated *Chlamydomonas* cells (negative control), hot-water treated cells (positive control) and cells exposed for 2 h and 24 h to the four Fe-containing materials ( $500 \, \mathrm{mg} \, \mathrm{L}^{-1}$ ) were visualised using an AxioImager microscope (Zeiss, Germany) equipped with an AxioCam ICc1 digital camera and AxioVision SE64 software.

#### 2.8. Statistical analysis

Differences in the effects observed for *Chlamydomonas* exposed to different particle concentrations and unexposed *Chlamydomonas* were tested using ANOVA and Dunnett's test (GraphPad PRISM, USA), with significance levels set at \* P < 0.05, \*\* P < 0.01 and \*\*\* P < 0.001.

#### 3. Results

## 3.1. Characterisation of Fe-containing materials in the algal exposure medium

Nano-Goethite had the smallest Z-average hydrodynamic size (207–288 nm) of all the materials tested, being about 3.5 times smaller than that of Fe-zeolites (Table 2). For Carbo-Iron® and FerMEG12, Z-average size ranged from 1289 to 2874 nm and 3726–4974 nm, respectively, with higher values for FerMEG12 being due to agglomeration. No significant difference in Z-average size was observed at 2 h and 24 h after dispersion in the algal exposure medium (Table 2). FerMEG12 and Nano-Goethite both displayed monomodal size distributions, while Carbo-Iron® and Fe-zeolites both showed bimodal number- and scattered light intensity-based size distributions (Fig. S7).

With the exception of FerMEG12, which showed positive zeta potential values (+ 5 mV) at high concentrations (500 mg  $L^{-1}$ ), all other materials displayed negative Zeta potentials (- 8 to - 35 mV; Fig. 1), with no significant difference in Zeta potential at 2 h and 24 h for all materials. For all particle types, negative values increased slightly as the concentration increased.

Growth medium pH values ranged between 7 and 8 for all *Chlamydomonas* samples following dispersion of the Fe materials (Fig. S8A). In the presence of Carbo-Iron®, Fe-zeolites and Nano-Goethite, pH values were comparable with those in the absence of Fe-containing materials. The pH of algal medium containing FerMEG12, however, increased to 8 at highest concentrations (500 mg L $^{-1}$ ). ORP values for cultures without particles were in the range of + 80 to + 210 mV (Fig. S8B). In contrast, the ORP for FerMEG12 ranged between - 200 and - 300 mV at time 0, but was comparable with the other particle types at + 80 to + 180 mV at 24 h.

#### 3.2. Effect of Fe-containing materials on growth rate and cell morphology

Growth rate in the presence of Fe-containing materials was not

**Table 2**Z-averaged particle size determined in algal growth medium after 2 h and 24 h. The results represent the average of three replicated experiments.

Particles	Z-average size after $2 h (nm \pm SD)$			
	$10\mathrm{mg}\mathrm{L}^{-1}$	$50\mathrm{mg}\mathrm{L}^{-1}$	500 mg L <sup>-1</sup>	
FerMEG12	4076 ± 320	3726 ± 580	4608 ± 243	
Carbo-Iron®	$2874 \pm 1005$	$1515 \pm 183$	$1289 \pm 26$	
Fe-zeolites	845 ± 114	$810 \pm 88$	$789 \pm 41$	
Nano-Goethite	$254 \pm 1$	$288 \pm 80$	$233 \pm 11$	
	Z-average size after 24 h (nm ± SD)			
FerMEG12	4974 ± 1426	$4721 \pm 380$	$4426 \pm 340$	
Carbo-Iron®	$2037 \pm 656$	$1643 \pm 174$	$1326 \pm 16$	
Fe-zeolites	$977 \pm 420$	798 ± 114	$856 \pm 58$	
Nano-Goethite	$207 \pm 3$	$251\pm6$	$245 \pm 2$	

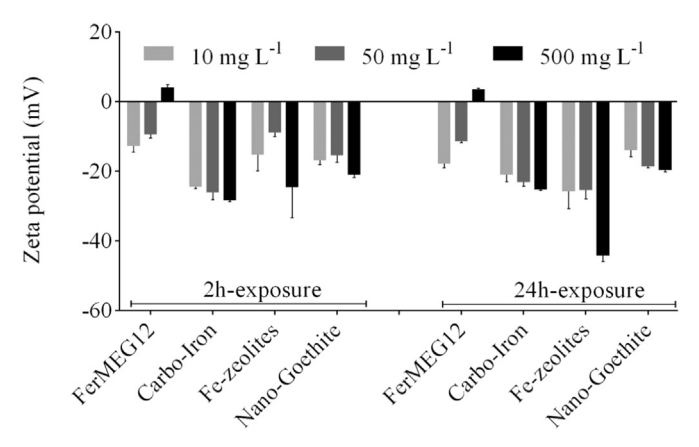


**Fig. 1.** Zeta-potential of particle surfaces at different concentrations after 2 h and 24 h dispersed in algal growth medium. Error bars = standard deviation of triplicate samples.

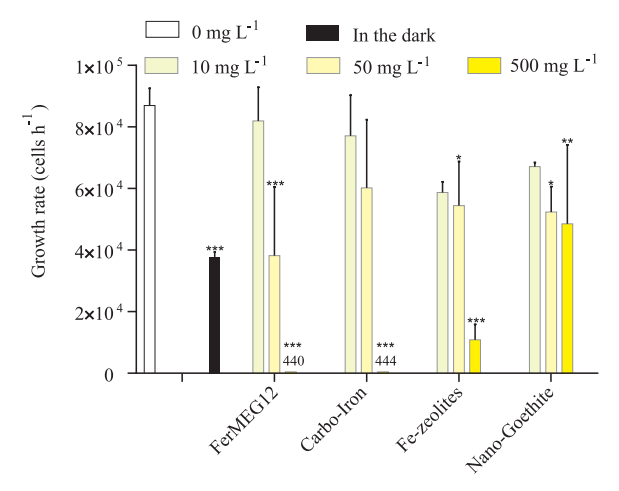


Fig. 2. Effect of four particle types on algal growth rate (cells  $h^{-1}$ ) measured with FCM. Exposure conditions: FerMEG12, Carbo-Iron\*, Fe-zeolites and Nano-Goethite at concentrations of 10, 50, 500 mg L $^{-1}$ . The error bars represent the standard deviation of triplicate samples. Significance levels \* P < 0.05, \*\* P < 0.01, and \*\*\* P < 0.001.

reduced compared with growth rate in the dark without particles  $(3.8\times10^4~{\rm cells\,h^{-1}},~P<0.001;~{\rm Fig.~2}).$  In general, growth rate decreased gradually as Fe-material concentration increased. At  $500~{\rm mg\,L^{-1}},~{\rm growth}$  rate was reduced to  $4.4\times10^2~{\rm cells\,h^{-1}}$  for FerMEG12 and Carbo-Iron® (P < 0.001),  $1.1\times10^4~{\rm cells\,h^{-1}}$  for Fezeolites (P < 0.001) and  $4.9\times10^4~{\rm cells\,h^{-1}}$  for Nano-Goethite (P < 0.01) compared to the unexposed control (8.7  $\times10^4~{\rm cells\,h^{-1}}).$  When algal cells were grown in the presence of  $50~{\rm mg\,L^{-1}}$  of FerMEG12, growth rate was reduced significantly (P < 0.001), while Fe-zeolite and Nano-Goethite both showed a slightly lower but still significant negative effect on growth rate (P < 0.05). The same concentration of Carbo-Iron®, however, appeared to have no effect on growth rate. At the lowest particle concentration (10  ${\rm mg\,L^{-1}}$ ), algal growth rate was comparable with that for the untreated control culture (Fig. 2) for all test materials.

Microscopic analysis revealed that algal cells were often associated with particle agglomerates following short-term (2 h) exposure with FerMEG12 and Carbo-Iron\* but not with Fe-zeolites and Nano-Goethite (Fig. S9A, C, E, G). Interestingly, after 24 h exposure, all algal cells tended to detach from the agglomerates and revert to a dispersed single-cell state (Fig. S9).

## 3.3. Effect of Fe materials on algal chlorophyll fluorescence and PSII efficiency

The percentage of cells with altered chlorophyll fluorescence

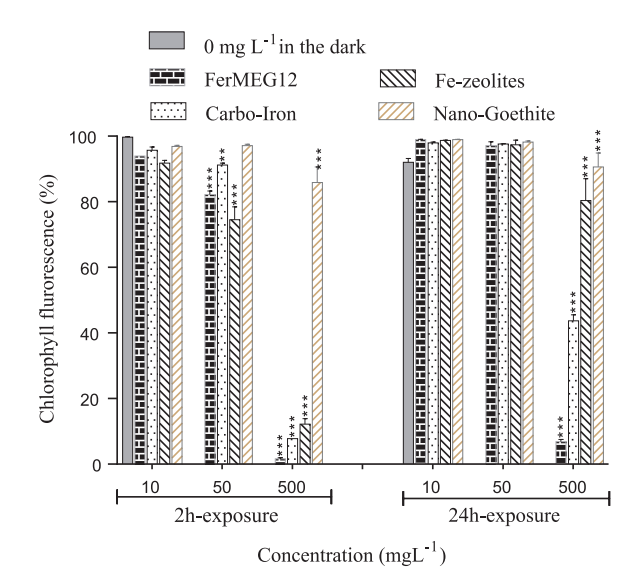


**Fig. 3.** Effect of Fe materials on chlorophyll fluorescence in *Chlamydomonas* cells. Exposure conditions: FerMEG12, Carbo-Iron\*, Fe-zeolites and Nano-Goethite at concentrations of 10, 50, 500 mg L $^{-1}$ , duration 2 h and 24 h. The chlorophyll fluorescence of unexposed control represents 100%. The error bars represent the standard deviation of triplicate samples. Significance levels \* P < 0.05, \*\* P < 0.01, and \*\*\* P < 0.001.

(extracted from FCM channel FL3; Fig. S6) increased significantly after  $2\,h$  exposure to FerMEG12, Carbo-Iron® and Fe-zeolites at concentrations of 50 and 500 mg L $^{-1}$ , and to Nano-Goethite at concentrations of 500 mg L $^{-1}$  only (85.6%). Although less pronounced, the same trends were observed after 24 h exposure (Fig. 3).

The above observations were consistent with an effect on PSII QY, an indicator of photosynthetic efficiency. PSII QY values for *Chlamydomonas* exposed to 10 mg L<sup>-1</sup> of each material for 2 h and 24 h were comparable with those for unexposed controls (Fig. 4). In contrast, exposure to FerMEG12 for 24 h at 50 mg L<sup>-1</sup> resulted in a reduction of PSII QY. Fe-zeolites and Nano-Goethite at 500 mg L<sup>-1</sup> caused a significant increase in PSII QY after 2 h exposure but not after 24 h. The dark colour of FerMEG12 and Carbo-Iron® (500 mg L<sup>-1</sup>) precluded reliable measurements of QY, thus control samples kept under dark

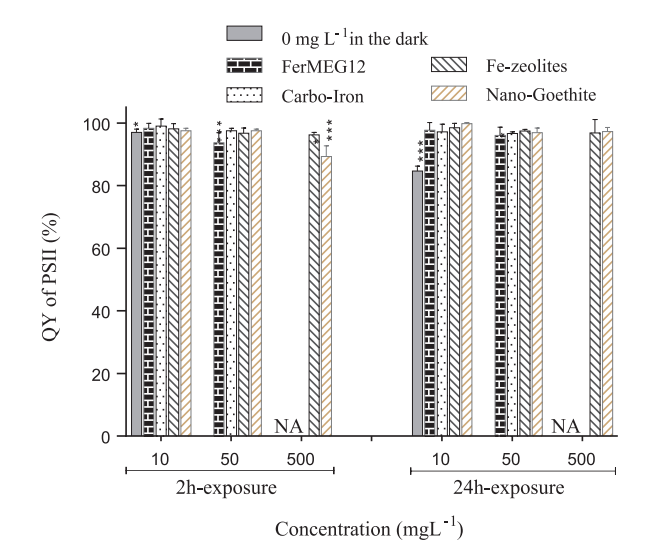


**Fig. 4.** Effect of Fe materials on the quantum yield (QY) of photosystem II (%) of *Chlamydomonas* after 2 h and 24 h exposure to Fe-NMs at 0, 10 and 50 mg L $^{-1}$  (FerMEG12, Carbo-Iron\*) and 0, 10, 50 and 500 mg L $^{-1}$  (Fe-zeolites, Nano-Goethite). Grey bars are control algae grown without nanoparticles in the dark. The control without particles represents 100%. NA = not analysed as the dark colour induced by the particle suspensions interfered with measurement. The error bars represent the standard deviation of triplicate samples. Significance levels \* P < 0.05, \*\* P < 0.01, and \*\*\* P < 0.001.

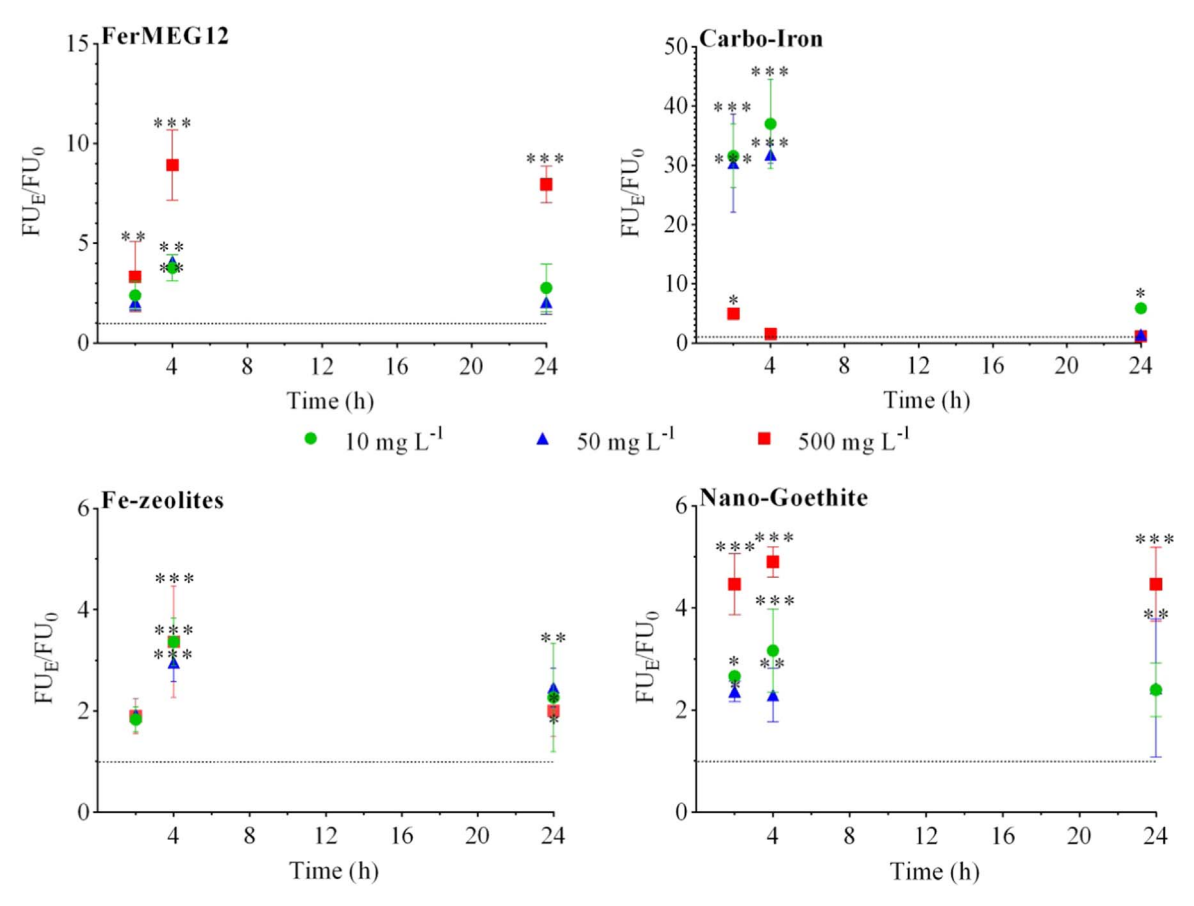


Fig. 5. Fluorescence unit (FU) ratios ( $FU_E/FU_0$ ) of ROS production in *Chlamydomonas* cells after 2 h and 24 h exposure to FerMEG12, Carbo-Iron\*, Fe-zeolites and Nano-Goethite at concentrations of 10 (green circle), 50 (blue up-triangle) and 500 (red square) mg L<sup>-1</sup>.  $FU_E$ : florescence unit of exposed algae to Fe-NMs,  $FU_0$ : non-exposed *Chlamydomonas* cultures. The dotted line (—) represents the control and the error bars represent the standard deviation of triplicate samples. Note the different y-axis scales. Significance levels \* P < 0.05, \*\* P < 0.01, and \*\*\* P < 0.001. (For interpretation of the references to color in this figure legend, the reader is referred to the web version of this article.)

conditions mimicked the shading effect. In the complete dark, algal chlorophyll fluorescence was progressively reduced to 92.0% (P < 0.001) over 24 h. Correspondingly, PSII QY was significantly reduced after 2 and 24 h (Fig. 4).

## 3.4. Effect of Fe materials on cellular ROS generation and membrane integrity

There was no clear trend in ROS production in the particle-treated Chlamydomonas sp. (Fig. 5). FerMEG12 caused a significant increase in ROS at 500 mg L<sup>-1</sup> after 2 h, and at all concentrations after 4 h. After 24 h, however, ROS formation was reduced at lower exposure concentrations (10,  $50 \text{ mg L}^{-1}$ ) to levels comparable with untreated cells, but remained higher at 500 mg L<sup>-1</sup>. Fe-zeolites, ROS generation was very low compared to FerMEG12 and Carbo-Iron®. While it increased slightly after 4 h it decreased again after 24 h, though remaining higher than the untreated control. Carbo-Iron® ROS levels increased rapidly when cells were exposed to 10 and 50 mg  $L^{-1}$  of the material, attaining a maximum at 4 h. At the highest Carbo-Iron® concentrations (500 mg L<sup>-1</sup>), however, enhanced ROS generation was not observed after 4 h or 24 h exposure. Nano-Goethite at 500 mg L<sup>-1</sup> resulted in elevated ROS levels at all exposure durations. At the lowest concentration (10 mg L<sup>-1</sup>), enhanced ROS was observed after 2 h and increased after 4 h but was comparable with ROS in untreated cells after 24 h (Fig. 5).

Exposure to Fe-containing materials induced a relatively weak effect on algal membrane integrity. In agreement with the observed decrease in cell number and algal chlorophyll fluorescence, the percentage of cells with affected membrane integrity was higher after 2 h than after 24 h exposure for all the materials studied (Fig. 6). The percentage of unaffected cells should ideally be 100%; values ranged between 95% and 100%, however, due to the FCM gating strategy attempting to remove all particles. While the percentage of affected membranes was 30–40% for FerMEG12, 18% for Carbo-Iron®, 29% for Fe-zeolites and 10% for Nano-Goethite at concentrations of 10 and 50 mg L $^{-1}$  following exposure for 2 h, these percentages had all decreased to around 10% after 24 h exposure. Even at the highest concentration tested (500 mg L $^{-1}$ ), membrane integrity levels were moderate at 39% for FerMEG12, 25% for Carbo-Iron®, 25% for Fe-zeolites and 15% for Nano-Goethite. On the other hand, there was a significant difference in the proportion of damaged membranes after 2 h and 24 h exposure at high (500 mg L $^{-1}$ ) particle concentrations (Fig. 6).

#### 4. Discussion

#### 4.1. Main biological effects of Fe-containing materials

FerMEG12 appears to be most toxic to *Chlamydomonas* sp., as demonstrated by the significant effect on different biological endpoints at concentration higher than  $50 \, \mathrm{mg} \, \mathrm{L}^{-1}$ . Note, however, that algal growth rate in the presence of FerMEG12 increased, and other effects were less pronounced, after 24 h. This observation is in agreement with an earlier study showing that FerMEG12 caused a decrease in chlorophyll fluorescence right after onset of acute effect on *Pseudomonas subcapitata* but after 48 h incubation, algal population recovered and the growth rate was similar or even higher than the non-exposed controls (Hjorth et al., 2017). Other reactive materials containing Fe(0), such as NANOFER STAR and NANOFER 25S, induced growth inhibition in marine

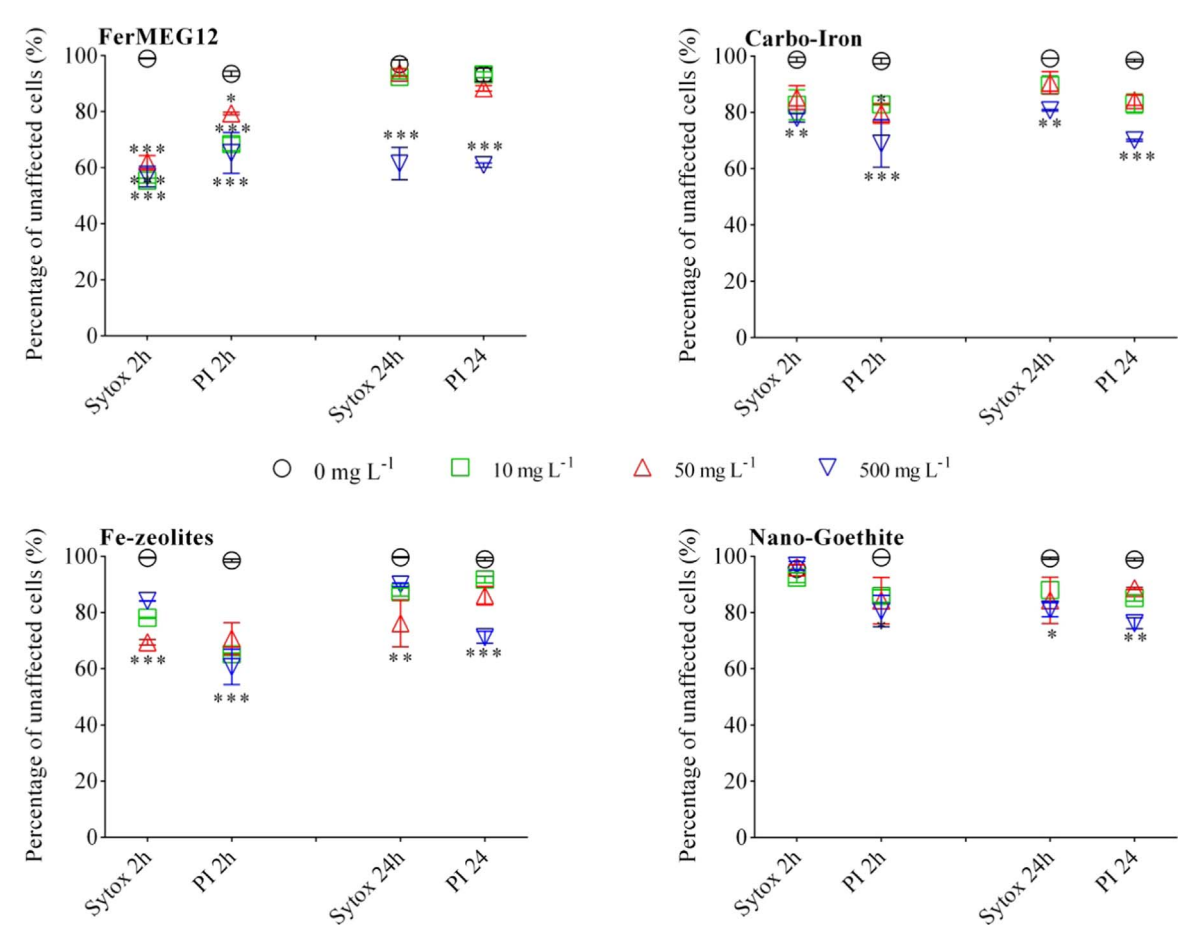


Fig. 6. Influence of the Fe materials on the membrane integrity of *Chlamydomonas* cells after 2 h and 24 h exposure to FerMEG12, Carbo-Iron®, Fe-zeolites and Nano-Goethite at concentrations of 10 (green square), 50 (red up-triangle) and 500 mg L $^{-1}$  (blue down-triangle). The error bars represent the standard deviation of triplicate samples. Significance levels \* P < 0.05, \*\* P < 0.01, and \*\*\* P < 0.001. (For interpretation of the references to color in this figure legend, the reader is referred to the web version of this article.)

microalga Isochrysis galbana at  $3\,\mathrm{mg}\,\mathrm{L}^{-1}$  (NANOFER 25S) or had no effect (NANOFER STAR up to  $100 \, \text{mg} \, \text{L}^{-1}$  or dissolved Fe at concentrations  $< 50 \, \text{mg L}^{-1}$ ) (Keller et al., 2012). The lowest observed effect concentration of Fe(II) and Fe(III) exposed to P. subcapitata was  $5 \text{ mg L}^{-1}$  and  $25 \text{ mg L}^{-1}$ , respectively, after 96 h (Keller et al., 2012). ZVI toxicity can also be influenced by corrosion and transformation processes, ferrous ion release and oxygen consumption (Chen et al., 2013; Zhu et al., 2012). Furthermore, transition metals (Fe) can participate in one-electron oxidation-reduction reactions producing ROS, which can have direct toxic effects on living organisms (Crane and Scott, 2012; Ševců et al., 2011; Schiwy et al., 2016). Surprisingly, the Carbo-Iron -induced generation of elevated ROS in the present study was higher at lower concentrations (50 mg L<sup>-1</sup>) than at higher concentration (500 mg  $L^{-1}$ ). One explanation may be that, at 500 mg  $L^{-1}$ , embedded Fe(0) has a longer life-span as oxygen dissolved in the exposure medium would be 'caught', leading to reduced release of Fe(II) and lowered ROS at 24 h. Moreover, the activated carbon carrier could effectively scavenge any ROS-initiators. nZVI toxicity strongly depends on the percentage of ZVI used and on the surface coating (El-Temsah et al., 2016, 2017). FerMEG12, for example, with 80% Fe(0), was without surface passivation and displayed higher toxicity to Chlamydomonas sp. than the other Fe-containing materials. This could be due to higher release of Fe(II) followed by higher uptake by algal cells, causing oxidative stress via the classic Fenton reaction (Lee et al., 2008; Ševců et al., 2011). Active defence mechanisms against ROS are, however, a prerequisite for aerobic organisms such as algae (Schwab et al., 2011; Cheloni et al., 2014). Even though both Fe-zeolites and Nano-Goethite generated cellular ROS, their levels were considerably lower than those in FerMEG12 and Carbo-Iron® exposure reflecting the

significant role of ZVI in induction of oxidative stress in algal cultures. On the other side, modified Fe(III)-zeolite inhibited *Chlamydomonas vulgaris* growth, probably due to the formation of ROS (Pavlíková et al., 2010). Of the studied materials Nano-Goethite weakly affected algal membranes, and affected chlorophyll fluorescence at the highest concentration (500 mg L<sup>-1</sup>) only. At the micro-scale, goethite is commonly found in the natural environment and there have been no previous reports of toxicity to microorganisms (Cooper et al., 2003).

#### 4.2. Other factors involved in ecotoxicity effects

Each of the Fe-containing materials tested has its own specific and unique properties for targeted application. Some of these characteristics should be taken into account, however, when undertaking ecotoxicity studies, e.g.:

- (1) The dark colour of FerMEG12 and Carbo-Iron®, and the colouration of Nano-Goethite at higher concentrations (500 mg L<sup>-1</sup>), resulted in shading of the algal cells (Figs. S2 and S3). Algal toxicity tests have revealed that shading can considerably influence assessment of potential toxicity at high exposure concentrations (Hjorth et al., 2015; Sørensen et al., 2016). In one study, it was shown that ZVI shading reduced algal growth to a higher extent than other toxicity mechanisms (Schiwy et al., 2016). Shaded algal cells need more chlorophyll to acquire enough photons for photosynthesis (Nielsen and Jørgensen, 1968); hence, they rapidly synthesise chlorophyll as an adaptation to darker conditions (Schwab et al., 2011; Hjorth et al., 2015).
- (2) The larger size of FerMEG12 and Carbo-Iron® (whether in their

- original state or due to agglomeration) and consequent sedimentation could reduce their effect on *Chlamydomonas* sp. This is consistent with the increased toxicity of FerMEG12 agglomerates at higher Fe concentrations to oligochaeta *Lumbriculus variegatus* due to particle sedimentation compared with *Daphnia magna*, which can move in the water column (Hjorth et al., 2017).
- (3) Other constituents within the Fe-containing materials may also need to be considered in toxicity studies. FerMEG12, for example, had a lower Fe-mass referred surface than Carbo-Iron® and was more hydrophobic (due to glycol on its surface). It might be expected, therefore, that the amount of Fe-ions released in the vicinity of the particles will differ. With higher particle concentration, particle-algae-interactions are suspected to be more pronounced, with algae possibly attaching to the glycol-film on FeMEG12 and AC in Carbo-Iron® materials.
- (4) Fe-zeolites have two phases of in situ application: a sorption phase following particle injection to the aquifer and, after sorption is complete, a flush of  $H_2O_2$  is applied, which leads to hydroxyl radical formation (Fenton-like reaction), to regenerate the particles and oxidise contaminants. It is quite probable that some microorganisms would be destroyed during this second phase. In this study, however, the Fe-zeolites were treated as representing an accidental introduction into the environment (e.g. by a spill reaching a waterbody), where the  $H_2O_2$  oxidation phase does not play a role.
- (5) Chemical-physical parameters: ORP values in algal cultures treated with FerMEG12 (50–500 mg L<sup>-1</sup>) ranged from −300 mV to −200 mV (Fig. S8), suggesting that algal cells were subjected to unfavourable reducing conditions in the growth medium at the beginning of the experiment. These low ORP values could have negatively affected algal density (Wang et al., 2014). There is no evidence that pH affected the algal cells as it remained within the optimal growth range (pH 7 − 8, Fig. S8) for *Chlamydomonas* (Messerli et al., 2005). Nevertheless, the zeta-potential of FerMEG12 in exposure medium reached values close to zero mV, or positive values at concentrations of 500 mg L<sup>-1</sup>, suggesting facilitated interaction of positively charged material surfaces with negatively charged algal cell surfaces.
- (6) Even though there was no direct evidence that the shape of the Fecontaining materials affected algal cells, the percentage of membranes damaged by FerMEG12 was higher than that for other materials. It can thus be hypothesised that FerMEG12, having a flakelike appearance with rough, sharp edges on surface (Fig. S1), might impair cell membranes directly.

#### 5. Conclusions

Investigation of four Fe-containing materials (FerMEG12, Carbo-Iron®, Fe-zeolites and Nano-Goethite) showed that biological effects on *Chlamydomonas* sp. were non-significant at low concentrations (10 and 50 mg L<sup>-1</sup>), being similar or below those expected when such materials enter aquatic environments through accidental spills. Negative effects were observed at high concentration (500 mg L<sup>-1</sup>), and especially for FerMEG12, which contained the highest proportion of reactive ZVI (80%). Overall, all effects tended to be less pronounced after 24 h at all concentrations, suggesting rapid recovery of the algal culture. High concentrations, in the exposure medium, however, caused problems when evaluating test endpoints, particularly as regards dark colouration resulting in a shading effect, agglomeration and sedimentation and consequent problem with assessment of concentration-based effects. On the other hand, agglomeration and sedimentation should be considered typical behaviour for these materials in the environment.

#### Acknowledgements

This research was supported by the European Union's Seventh

Framework Programme for research, technological development and demonstration under Grant Agreement no. 309517. Further support was provided to N. Nguyen and A. Ševců from the Ministry of Education, Youth and Sport (CZ project no. LO1201 and NanoEnvi project no. LM2015073) and from the Technology Agency of the Czech Republic (Project no. TE01010218). V. Slaveykova and N. von Moos received funding from the Swiss National Science Foundation (NRP 64: on the Opportunities and Risk of Nanomaterials, Project no. 406440-131280).

#### Conflict of interest

The authors declare that they have no conflict of interest.

#### Appendix A. Supporting information

Supplementary data associated with this article can be found in the online version at http://dx.doi.org/10.1016/j.ecoenv.2018.02.027.

#### References

- Adeleye, A.S., Stevenson, L.M., Su, Y., Nisbet, R.M., Zhang, Y., Keller, A.A., 2016. Influence of phytoplankton on fate and effects of modified zerovalent iron nanoparticles. Environ. Sci. Technol. 50, 5597–5605.
- Auffan, M., Achouak, W., Rose, J., Roncato, M.A., Chanéac, C., Waite, D.T., Masion, A., Woicik, J.C., Wiesner, M.R., Bottero, J.Y., 2008. Relation between the redox state of iron-based nanoparticles and their cytotoxicity toward *Escherichia coli*. Environ. Sci. Technol. 42. 6730–6735.
- Bardos, P., Bone, B., Černík, M., Elliott, D.W., Jones, S., Merly, C., 2015. Nanoremediation and international environmental restoration markets. Remediat. J. 26, 101–108.
- Bleyl, S., Kopinke, F.D., Mackenzie, K., 2012. Carbo-Iron-synthesis and stabilization of Fe (0)-doped colloidal activated carbon for in situ groundwater treatment. Chem. Eng. J. 191. 588–595.
- Bosch, J., Heister, K., Hofmann, T., Meckenstock, R.U., 2010. Nanosized iron oxide colloids strongly enhance microbial iron reduction. Appl. Environ. Microbiol. 76, 184-180
- Braunschweig, J., Bosch, J., Meckenstock, R.U., 2013. Iron oxide nanoparticles in geomicrobiology: from biogeochemistry to bioremediation. New Biotechnol. 30, 793–802
- Cheloni, G., Cosio, C., Slaveykova, V.I., 2014. Antagonistic and synergistic effects of light irradiation on the effects of copper on *Chlamydomonas reinhardtii*. Aquat. Toxicol. 155C, 275–282.
- Cheloni, G., Marti, E., Slaveykova, V.I., von Moos, N., Maillard, L., Slaveykova, V.I., Regier, N., Cosio, C., von Moos, N., Slaveykova, V.I., 2016. Interactive effects of copper oxide nanoparticles and light to green alga *Chlamydomonas reinhardtii*. Aquat. Toxicol. 170, 120–128.
- Chen, P.-J.J., Wu, W.-L.L., Wu, K.C.-W.W., 2013. The zerovalent iron nanoparticle causes higher developmental toxicity than its oxidation products in early life stages of medaka fish. Water Res. 47, 3899–3909.
- Cooper, D.C., Picardal, F.W., Schimmelmann, A., Coby, A.J., 2003. Chemical and biological interactions during nitrate and goethite reduction by *Shewanella putrefaciens* 200. Appl. Environ. Microbiol. 69, 3517–3525.
- Crane, R.A., Scott, T.B., 2012. Nanoscale zero-valent iron: future prospects for an emerging water treatment technology. J. Hazard. Mater. 211–212, 112–125.
- Davies, K.J., A Davies, K.J., Percy, E., 2000. Critical review oxidative stress, antioxidant defenses, and damage removal, repair, and replacement systems. IUBMB Life 50, 279–289.
- Nielsen, E.S., Jørgensen, E.G., 1968. The adaptation of plankton algae. Physiol. Plant. 21, 423–427.
- El-Temsah, Y.S., Sevcu, A., Bobcikova, K., Cernik, M., Joner, E.J., 2016. DDT degradation efficiency and ecotoxicological effects of two types of nano-sized zero-valent iron (nZVI) in water and soil. Chemosphere 144, 2221–2228.
- Franqueira, D., Orosa, M., Torres, E., Herrero, C., Cid A., 2000. Potential use of flow cytometry in toxicity studies with microalgae. Sci. Total Environ. 247, 119–126.
- Gillies, G., Mackenzie, K., Kopinke, F.D., Georgi, A., 2016. Fluorescence labelling as tool for zeolite particle tracking in nanoremediation approaches. Sci. Total Environ. 550, 820–826.
- Gillies, G., Rukmini, R., Kopinke, F.-D., Georgi, A., 2017. Suspension stability and mobility of Trap-Ox Fe-zeolites for in-situ nanoremediation. J. Colloid Interface Sci. 501, 311–320.
- Gonzalez-Olmos, R., Kopinke, F.D., Mackenzie, K., Georgi, A., 2013. Hydrophobic Fezeolites for removal of MTBE from water by combination of adsorption and oxidation. Environ. Sci. Technol. 47, 2353–2360.
- Guillard, R.R.L., Lorenzen, C.J., 1972. Yellow-green algae with chlorophyllide c. J. Phycol. 8, 10–14.
- Hjorth, R., Sørensen, S.N., Olsson, M.E., Baun, A., Hartmanny, N.B., 2015. A certain shade of green: can algal pigments reveal shading effects of nanoparticles? Integr. Environ. Assess. Manag. 11, 719–728.
- Hjorth, R., Coutris, C., Nguyen, N., Sevcu, A., Baun, A., Joner, E., 2017. Ecotoxicity

- testing and environmental risk assessment of iron nanomaterials for sub-surface remediation – recommendations from the FP7 project NanoRem. Chemosphere 182, 525–531.
- Keller, A.A., Garner, K., Miller, R.J., Lenihan, H.S., 2012. Toxicity of nano-zero valent iron to freshwater and marine organisms. PLoS One 7, 1–10.
- Klaine, S.J., Alvarez, P.J.J., Batley, G.E., Fernandes, T.F., Handy, R.D., Lyon, D.Y., Mahendra, S., McLaughlin, M.J., Lead, J.R., 2008. Nanomaterials in the environment: behavior, fate, bioavailability, and effects. Environ. Toxicol. Chem. 27, 1825–1851.
- Köber, R., Hollert, H., Hornbruch, G., Jekel, M., Kamptner, A., Klaas, N., Maes, H., Mangold, K.-M., Martac, E., Matheis, A., Paar, H., Schäffer, A., Schell, H., Schiwy, A., Schmidt, K.R., Strutz, T.J., Thümmler, S., Tiehm, A., Braun, J., 2014. Nanoscale zerovalent iron flakes for groundwater treatment. Environ. Earth Sci. 72, 3339–3352.
- Lee, C., Kim, J.Y., Lee, W., Il, Nelson, K.L., Yoon, J., Sedlak, D.L., 2008. Bactericidal effect of zero-valent iron nanoparticles on Escherichia coli. Environ. Pollut. 13, 4927–4933.
- Lei, C., Zhang, L., Yang, K., Zhu, L., Lin, D., 2016. Toxicity of iron-based nanoparticles to green algae: effects of particle size, crystal phase, oxidation state and environmental aging. Environ. Pollut. 218, 505–512.
- Mackenzie, K., Bleyl, S., Georgi, A., Kopinke, F.D., 2012. Carbo-Iron An Fe/AC composite As alternative to nano-iron for groundwater treatment. Water Res. 46, 3817–3826.
- Mackenzie, K., Bleyl, S., Kopinke, F.D., Doose, H., Bruns, J., 2016. Carbo-Iron as improvement of the nanoiron technology: from laboratory design to the field test. Sci. Total Environ. 563–564, 641–648.
- Maxwell, K., Johnson, G.N., 2000. Chlorophyll fluorescence–a practical guide. J. Exp. Bot. 51, 659–668.
- Messerli, M.A., Amaral-Zettler, L.A., Zettler, E., Jung, S.-K., Smith, P.J.S., Sogin, M.L., 2005. Life at acidic pH imposes an increased energetic cost for a eukaryotic acidophile. J. Exp. Biol. 208, 2569–2579.
- Mueller, N.C., Braun, J., Bruns, J., Černík, M., Rissing, P., Rickerby, D., Nowack, B., 2012.
  Application of nanoscale zero valent iron (NZVI) for groundwater remediation in Europe. Environ. Sci. Pollut. Res. 19, 550–558.
- Pavlíková, S., Šerše, F., Jesenák, K., Gáplovská, K., Gabriel, Č., 2010. Efficacy of modified natural zeolites in the protection against the damaging effect of 4-chlorophenol on algal growth. Fresenius Environ. Bull. 19, 3055–3058.

- Ribas, D., Cernik, M., Martí, V., Benito, J.A., 2016. Improvements in nanoscale zerovalent iron production by milling through the addition of alumina. J. Nanopart. Res. 18, 191
- Schiwy, A., Maes, H.M., Koske, D., Flecken, M., Schmidt, K.R., Schell, H., Tiehm, A., Kamptner, A., Thümmler, S., Stanjek, H., Heggen, M., Dunin-Borkowski, R.E., Braun, J., Schäffer, A., Hollert, H., 2016. The ecotoxic potential of a new zero-valent iron nanomaterial, designed for the elimination of halogenated pollutants, and its effect on reductive dechlorinating microbial communities. Environ. Pollut. 216, 1–9.
- Schwab, F., Bucheli, T.D., Lukhele, L.P., Magrez, A., Nowack, B., Sigg, L., Knauer, K., 2011. Are carbon nanotube effects on green algae caused by shading and agglomeration? Environ. Sci. Technol. 45, 6136–6144.
- Ševců, A., El-Temsah, Y.S., Filip, J., Joner, E.J., Bobčíková, K., Černík, M., 2017. Zerovalent iron particles for PCB degradation and an evaluation of their effects on bacteria, plants, and soil organisms. Environ. Sci. Pollut. Res. 24, 21191–21202.
- Ševců, A., El-Temsah, Y.S., Joner, E.J., Černík, M., 2011. Oxidative stress induced in microorganisms by zero-valent iron nanoparticles. Microbes Environ. 26, 271–281.
- Sharma, V.K., Chen, L., Marsalek, B., Zboril, R., O'Shea, K.E., Dionysiou, D.D., 2016. Iron based sustainable greener technologies to treat cyanobacteria and microcystin-LR in water. Water Sci. Technol. Water Supply 17, 107–114.
- Sørensen, S.N., Engelbrekt, C., Lützhøft, H.H., Jiménez-Lamana, J., Noori, J.S., Alatraktch, F.A., Delgado, C.G., Slaveykova, V.I., Baun, A., 2016. A multi-method approach for disclosing algal toxicity of platinum nanoparticles. Environ. Sci. Technol. 19, 10635–10643.
- Soukupova, J., Zboril, R., Medrik, I., Filip, J., Safarova, K., Ledl, R., Mashlan, M., Nosek, J., Cernik, M., 2015. Highly concentrated, reactive and stable dispersion of zero-valent iron nanoparticles: direct surface modification and site application. Chem. Eng. J. 262, 813–822.
- Szivák, I., Behra, R., Sigg, L., 2009. Metal-induced reactive oxygen species production in Chlamydomonas reinhardtii (Chlorophyceae). J. Phycol. 45, 427–435.
- Wang, G., Li, X., Fang, Y., Huang, R., 2014. Analysis on the formation condition of the algae-induced odorous black water agglomerate. Saudi J. Biol. Sci. 21, 597–604.
- Zhu, X., Tian, S., Cai, Z., 2012. Toxicity assessment of iron oxide nanoparticles in Zebrafish (Danio rerio) early life stages. PLoS One 7, 1–6.